ADVANCED MATERIALS

Controlling the Microstructure of Monomolecular Layers**

Ultrathin Organic Films
Proteins in Thin Films
Fluorescence Microscopy
X-ray Scattering

By Helmuth Möhwald*

This review reports on the range of lateral structures which have been detected in ultrathin organic films using the newly-developed techniques of fluorescence microscopy and X-ray scattering, together with more conventional methods. A number of unusual low-dimensional ordering processes have been revealed. Hexagonal, lamellar or fractal domain structures are observed and shown to result from an interplay of electrostatic forces due to molecular alignment at interfaces, line energy between different phases and growth kinetics. On a molecular level the microstructure is distinguished by low coherence length of positional order but long coherence length concerning the orientation of crystallographic axes. It is demonstrated that the ideas presented are also relevant to adsorbate structures at interfaces and to the protein arrangement in monolayers.

1. Introduction

In designing a new organic material to perform a given function, it is typically necessary to link many atoms together in the desired spatial arrangement, using well-understood synthetic techniques. For some functions, however, these techniques are not sufficient, as it is also necessary to orient the resulting molecules. A number of different solutions to this problem are known, including crystallization, stretching or extrusion of a loaded polymer, dissolving the functional molecule in a liquid-crystalline matrix, and even the use of lithographically defined nm-sized holes. Here another technique is described, which achieves a very high degree of orientation of densely packed molecules. This technique, involving the principle of self-assembly and orientation of molecules at an interface, was first demonstrated by *Langmuir* and *Blodgett*.[1] It was extensively developed by the elegant work of *Kuhn* and coworkers who demonstrated the feasibility of building molecular machines.[2]

I will show that it is not only possible to design structures consisting of multilayers of ultrathin films with individual thickness of about 2 nm but that the lateral organization of molecules within these films can also be controlled. For this I will concentrate mainly on the monolayer at the air/water interface since the parameters in this system may be varied over a wide range, making it most suitable for understanding the underlying processes. These studies yield insight into new and interesting physics of two dimensions. This was possible by using the novel techniques of fluorescence microscopy and X-ray scattering together with established methods such as film balance and surface potential measurements as well as electron microscopy and spectroscopy. These techniques have become applicable to films as thin as 25 Å mainly due to the development of extremely sensitive TV cameras and of high intensity Synchrotron X-ray sources.

Experimental

Most of the experiments were performed with the phospholipids L-α-dimyristoylphosphatidic acid (DMPA) or L-α-dimyristoylphosphatidylethanolamine (DMPE) (Fluka). Both lipids are highly insoluble in water and form stable monolayers at the air/water interface when spread from solution (3 : 1 chloroform/methanol). The monolayer molecules are oriented, with the hydrophilic head groups pointing towards the water surface and the aliphatic chains towards the air. Varying the subphase ionic conditions by adding NaOH, NaCl (Fluka, p.a.), $CdCl_2$ (Merck), or other divalent ion salts or by binding divalent ions through addition of sodium ethylenediaminetetraacetate (EDTA, Sigma) affects the head group repulsion and thus also alters the microstructure.

As a more simple model compound arachidic acid $CH_3(CH_2)_{18}COOH$ (Fluka) was used. The charge-transfer salt *N*-docosylpyridinium-tetracyanoquinodimethane (Py-TCNQ) was obtained from *A. Barraud, J. Richard, A. Ruaudel-Teixier* and *M. Vandevyver* at Saclay, France; the diacetylenic lipid **1** ("Bronco") was a gift from *H. Ringsdorf*, Mainz. The positively charged surfactant dihexadecyldimethylammonium bromide used for studies of the adsorption of the water soluble disulfonated cyanine dye (Nippon, Kauko, Shikiso, NK 2012) was obtained from *M. Shimomura*, Tokyo, Japan. Concanavalin A (Con A) and dextran were obtained from Sigma. Water was Millipore filtered.

Fluorescence microscopy studies of the monolayer at the air/water interface were performed using a dedicated film balance with an integrated microscope. [3] Contrast is observed in the images leading to Figures 1 and 2 (section 2) since the dye probe NBD-PE **2** (dipalmitoyl-nitrobenzoxadiazol-phosphatidylethanolamine) incorporated into the monolayer in a molar con-

[*] Prof. Dr. H. Möhwald
Institut für Physikalische Chemie der Universität
Welder Weg 15, D-6500 Mainz (FRG)

[**] This report is based on the thesis works of my former and present coworkers at the Technische Universität München and Universität Mainz: *M. Flörsheimer, H. D. Göbel, H. Haas, W. M. Heckl, C. A. Helm, S. Kirstein, M. Lösche, A. Miller, R. Steitz* and *P. Tippmann-Krayer*. We enjoyed collaborations with *J. Als-Nielsen, K. Kjaer, W. Knoll, D. Möbius* and *E. Sackmann* and were supported by the Deutsche Forschungsgemeinschaft, Stiftung Volkswagenwerk and the Bundesministerium für Forschung und Technologie. I thank *I. R. Peterson* for critically reading the manuscript.

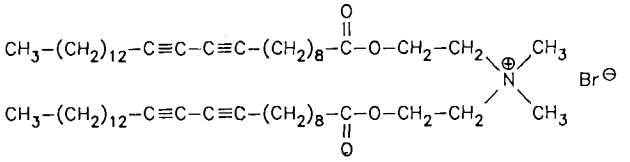

1, Bronco

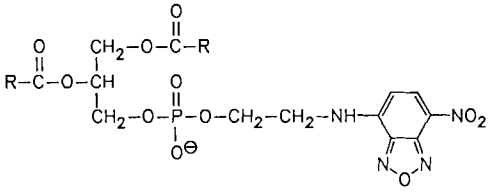

2, R = $(CH_2)_{14}CH_3$

centration below 1% is less soluble in the more ordered phase than in the fluid one. Different solubility in different phases also yields good contrast if a fluorescently labeled protein is used (Fig. 6, section 5). In a third variant of the technique, a water-soluble dye was not incorporated into the main monolayer, but instead formed extensive two-dimensional crystalline layers, or J-aggregates—aggregates of strongly interacting dyes in a coplanar arrangement—adjacent to it and under its influence. These J-aggregates typically had a high fluorescence yield and are shown in Figure 5.

X-ray scattering experiments with monolayers at the air/water interface were performed at the Synchrotron source of HASYLAB, DESY, Hamburg, in collaboration with *K. Kjaer* and *J. Als-Nielsen*, Risø, Denmark. [4-7] For measurements of X-ray diffraction with in-plane wave-vector transfer $Q_{\parallel} = \frac{4\pi}{\lambda} \sin\theta$ ($\lambda = 1.3815$ Å being the wavelength and θ the diffraction angle) the beam enters the surface at glancing incidence. For studies of X-ray reflection (normal wave-vector transfer) as a function of incidence angle α the height of the film balance at the sample stage of the diffractometer is varied. In these experiments the film balance with a pressure measuring system of the *Wilhelmy* type is embedded in a gas-tight housing.

For the electron micrographs, microscope grids were sandwiched between a glass slide and a formvar film, which was coated by vacuum deposition of 100 Å carbon and 50 Å SiO_2. Subsequently, the monolayer was deposited by the Langmuir-Blodgett technique. The observed contrast was due to differential charging of the crystalline and amorphous domains in the Philips EM 400 microscope. [8]

2. Domain Structure at the µm Level

Figure 1 gives a variety of fluorescence microscopic images observed after compression of a monolayer at the air/water interface to achieve a lateral pressure above π_c. The latter is defined from a distinct change in the slope of the isotherm "surface pressure as a function of area per molecule". It corresponds to the onset of the main phase transition of a lipid from a fluid to a more ordered state.[9] The transition is of first order and involves a change in the two-dimensional molecular density by up to 50%. In the denser phase the aliphatic tails are nearly parallel and in the all-*trans* configuration. Thus, the solubility is low for any impurity (e.g., the dye) and the phase appears dark under the fluorescence microscope. It is possible to observe coexistence of phases and to follow domain formation as a function of environmental parameters and time. Until recently, the domain shapes and superstructures presented in Figure 1 were completely unexpected. I will show by qualitative arguments that the periodic structures in Figure 1a, b form due to long-range electrostatic forces, whereas the shapes in Figure 1c, d are kinetically determined.

Electrostatic forces are a peculiar feature of this interfacial system and consist of two contributions: 1. Lipids have dissociable head groups and therefore the monolayer can be charged. The surface charge is counterbalanced either by ions in the subphase (e.g., divalent ions) that strongly bind to the head groups or by ions in the diffuse double layer. Thus, considering long range forces, the monolayer may be viewed as a dipolar sheet. The corresponding dipole moment can be calculated rather satisfactorily on the basis of Gouy-Chapman-Stern theory and varied via pH and ionic milieu.[10-13] 2. A qualitatively similar contribution results from the dipolar nature of the surfactant molecules. As the component of the dipole moment normal to the surface is not compensated due to the partial molecular alignment at the interface a total surface dipole moment results. This contribution is very difficult to assess because a molecule like a phospholipid contains many polar groups and the projection of these groups on the surface normal has to be known. Furthermore, due to the screening by water, the position relative to the water surface is very important. E.g., comparing a polar group above and below the water surface and a change in the dielectric constant from $\varepsilon(\text{water}) \approx 80$ to $\varepsilon(\text{hydrocarbon}) \approx 2$ the contribution of the group under water is reduced by a factor of $\varepsilon^2 \approx 6000$.[13] Therefore this contribution very sensitively depends on the local surface structure.

Despite this difficulty in theoretically quantifying these contributions their sum can be measured rather easily and accurately by surface potential measurements. According

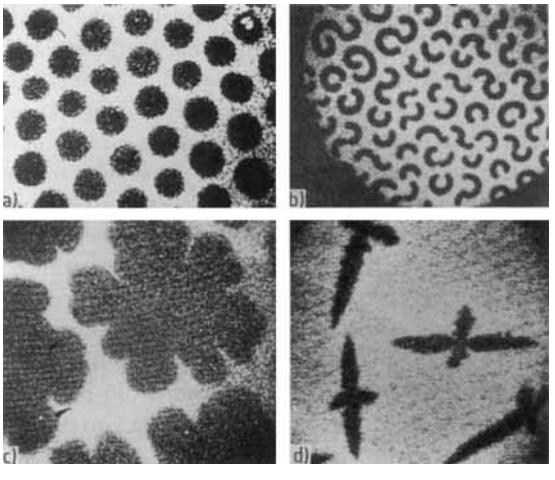

Fig. 1. Fluorescence micrographs of lipid monolayers containing about 1 mol% of the dye NBD-PE 2 in the phase coexistence region of a fluid (bright) and an ordered (dark) phase. The size of an image corresponds to 150 µm. a) DMPA, pH 11.3, 100 mM NaCl, 1 µM $CaCl_2$, $T = 10.5$°C; b) DMPA, 1 mol% cholesterol, pH 11.4, $T = 10$°C; c) DMPA, pH 5.5, $T = 20$°C; d) Bronco after a stepwise pressure increase, pH 5.5, $T = 20$°C.

to the Helmholtz equation the surface potential ΔV and the surface dipole moment are related by

$$\Delta V = \frac{\rho_D}{\varepsilon_0} \quad \text{(a)}$$

$\varepsilon_0 = 8.9 \times 10^{-12}$ C^2 m^{-2} N^{-1} and ρ_D is the dipole density normal to the surface. It is also possible to measure the differences in surface potential of fluid and ordered phases and then to calculate the differences in dipole density. These dipole density differences $\Delta\rho_D$, typically on the order of 100 mDebye nm^{-2} (and due to the difference in molecular density), enter into the calculation of long-range forces. To explain the hexagonal lattice of Figure 1a we have to answer two questions: 1. Why do individual domains repel one another over distances of several 10 μm? 2. Why do these domains exhibit uniform size?

Ad 1: As argued above the condensed phase domain can be considered as a dipolar disc of radius r with dipole moment P given by $P = \pi r^2 \Delta\rho_D$. The repulsive energy of two such discs at a center to center distance d can be estimated as[14]

$$W_{rep} = \frac{1}{4\pi\varepsilon\varepsilon_0 d^3} P^2 \quad \text{(b)}$$

Taking experimental numbers, it is easy to show that W_{rep} is much larger than kT (k = Boltzman const., T = absolute temperature), i.e., the repulsive energy is large enough to overcome any thermal motion.

Ad 2: Usually, for domain sizes above a critical radius r_c, the growth of larger domains is favored at the expense of smaller ones. This is due to the fact that the surface energy per molecule is smaller for a larger domain. The same holds also for a two-dimensional system where changes in surface energy may be ascribed to a line tension in the boundary between the ordered and fluid phases. Uniform domain size in an equilibrium situation therefore requires a force favoring small domains and thus counteracting line tension. Electrostatic forces, being of long range, yield such a contribution, because the energy density of a dipolar disc increases with size due to the dipolar repulsion of the individual molecules. Therefore one expects an equilibrium domain size. The quantitative calculation of the energy density, only logarithmically diverging with r, yields very poor agreement with experiment.[15] Furthermore, the domain dimensions can be varied via nucleation conditions indicating that they are nonequilibrium features.[16] On the other hand, these dimensions can be maintained over hours, and therefore the structure corresponds to a local minimum of free energy.

Hence the most plausible mechanism for formation of hexagonal superstructures is that a certain number of critical nuclei are formed during the initial stages of domain growth. These domains are of uniform size due to identical growth conditions, and they do not split into smaller pieces due to line tension, nor do they fuse due to electrostatic repulsion.

An interesting aspect left for further studies is to determine whether there is an interaction, probably inhibitory, between two growing domains. Electrostatic forces can also be considered to be responsible for formation of elongated domains. In the latter case electrostatic energy would be reduced since the mean distance between interacting molecular dipoles is increased. Elongation, however, requires additional line energy and therefore the balance between these forces determines an equilibrium shape. In the example shown in Figure 1b the electrostatic energy has been increased by increasing the pH (to 11) and reducing the temperature, and the line energy decreased by adding a small amount (1 mol%) of cholesterol.[17,18] Varying these parameters, one can reversibly change the domain width, which is an apparent equilibrium feature, and induce abrupt changes from lamellar to circular shapes. To understand the spiral shapes one additionally has to take into account molecular chirality.

In many cases domain formation at the air/water interface leads to smooth but irregular shapes that do not become circular even after hours (Fig. 1c). These shapes develop from much more convoluted domains similar to those of Figure 2. The sharpest edges are annealed due to the action of line tension whereas other edges remain.[19] The latter may be due to the presence of impurities which may be enriched in the areas between two protrusions of one domain. This locally reduces line tension, the force responsible for reduction of the domain boundary length.

In special cases one may also observe a pronounced anisotropy of domain morphology which, like in the case of a three-dimensional crystal, reflects the underlying crystallographic lattice.[20] For the case of the diacetylenic lipid Bronco one can show that there is a nearly orthorhombic

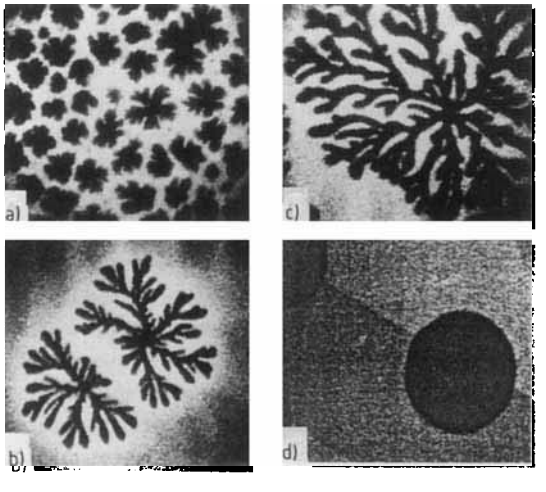

Fig. 2. Fluorescence micrographs of DMPE monolayers containing different concentrations c of a dye probe and at rather fast compression speed (1 Å^2 molecule^{-1} s^{-1}) a) $c = 6$ mol%, b) $c = 1.3$ mol%, c) $c = 0.3$ mol%. The shapes formed at high c do not anneal, whereas they become round at low c; see, e.g., Fig. 2d: $c = 0.7$ mol% after 20 min at constant pressure.

ADVANCED MATERIALS

lattice and that the two axes of preferred growth correspond to diagonals of the unit cell (see Fig. 1d).

These considerations show that the surface morphology strongly depends on growth kinetics, and useful structures may result. Thus it is very important to understand and to control the growth process. One way of doing this is to quickly vary the surface pressure and measure the development of domain size, domain shape, and pressure relaxation. Another possibility is to add impurities, of which the most convenient is the dye probe itself. Via analysis of the images, the impurity distribution can be measured.[19,21]

Typical images at different impurity (dye) concentrations are given in Figure 2. At very low dye concentrations highly convoluted structures are formed (Fig. 2b). These develop within times (<0.1 s) too short to be observed in our experiments. For intermediate dye concentrations (1 mol%) the structures are less intricate but their formation is slow enough to be followed (several seconds, Fig. 2c). For still higher dye concentrations many small domains result, again within very short times (Fig. 2a).

In the intermediate concentration range, where the development of the above mentioned parameters can be measured, the growth kinetics can be described within the framework of constitutional supercooling. During domain growth the impurities are less soluble in the ordered phase and are therefore enriched at the phase boundary.[19] There they reduce the melting temperature and thus inhibit the growth process. For further growth the process is controlled by impurity diffusion away from the interfacial area. The rate of diffusion to a protruding feature will be greater than that to an indentation leading to amplification of any initial roughness and ultimately to a highly folded boundary. Computer simulations on diffusion limited aggregation[22] reveal a self-similar structure with a fractal dimension of $f=1.5$ in accordance with the value determined by analysis of the images obtained immediately after a pressure jump.[21] f is measured and defined from the equation $M=R^f$, where M is the area of a domain within a radius R about its center. The rounding off at later times (see Fig. 2d) is again due to the influence of line tension. Since the latter is decreased for high impurity concentrations, one understands that structures formed at high dye concentrations never anneal within experimental times. On the other hand, since impurities favor the formation of critical nuclei this could explain the increase in the number of domains with impurity concentrations.

3. Microstructure at the Molecular Level

The variety of domain morphologies presented in Figure 1 is expected to correspond to qualitatively different crystallographic lattice structures. This has indeed been demonstrated in electron diffraction experiments with monolayers on solid supports. The diffraction pattern for a typical phospholipid like DMPE shows a hexagonally symmetric arrangement of rather broad spots and no second order diffraction peak.[12,23] It displays a hexagonal lattice with d_{10} spacings between 4.2 and 4.3 Å typical for vertically oriented aliphatic chains. The local crystallographic axes are parallel within one domain.

In the other extreme when domains with very sharp edges were observed, many narrow diffraction spots with lower than threefold symmetry are encountered. Examples for this are monolayers of the polymerized lipid[24] studied in Figure 1d, of cyanine dyes,[25] and of the Py-TCNQ[26] salt presented in Figure 3. For the latter, electron microscopy shows domains with straight faces and sharp edges. Due to charging by the intense beam applied for diffraction studies, the circular area from which the diffracted intensity was taken could be visualized. The pattern in the insert of Figure 3 shows a variety of spots that are still under more detailed analysis. Apparently in this case the very rigid and well-ordered structure is determined by the extended planar head groups that exhibit no flexibility.

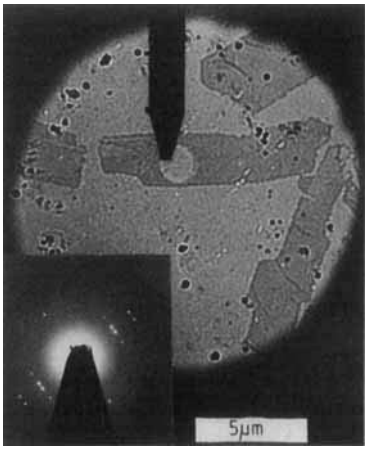

Fig. 3. Electron micrograph and electron diffraction pattern (insert) of a Py-TCNQ bilayer prepared by compression of a monolayer and transferred by the Langmuir-Blodgett technique.

To probe *in situ* the monolayer structure at the air/water interface X-ray diffraction[4,5,7] and reflexion studies[6,7] were performed with different monolayers at various surface pressures, densities, and subphase conditions. As an example, Figure 4 gives data for monolayers of the most frequently studied model compound arachidic acid. Figure 4a gives the intensity as a function of in plane scattering angle on increasing the surface pressure from bottom to top. Considering the variation of intensity and position with surface pressure one clearly observes three different regimes: I: For low surface pressures (high area per molecule, above A_1), the peak position is constant and the intensity increases with pressure. II: For intermediate areas per molecule, $A_s<A<A_1$, the intensity is constant but the position changes. III: Decreasing the area per molecule below A_s, the intensity abruptly increases whereas at higher pressures the line remains virtually unchanged.

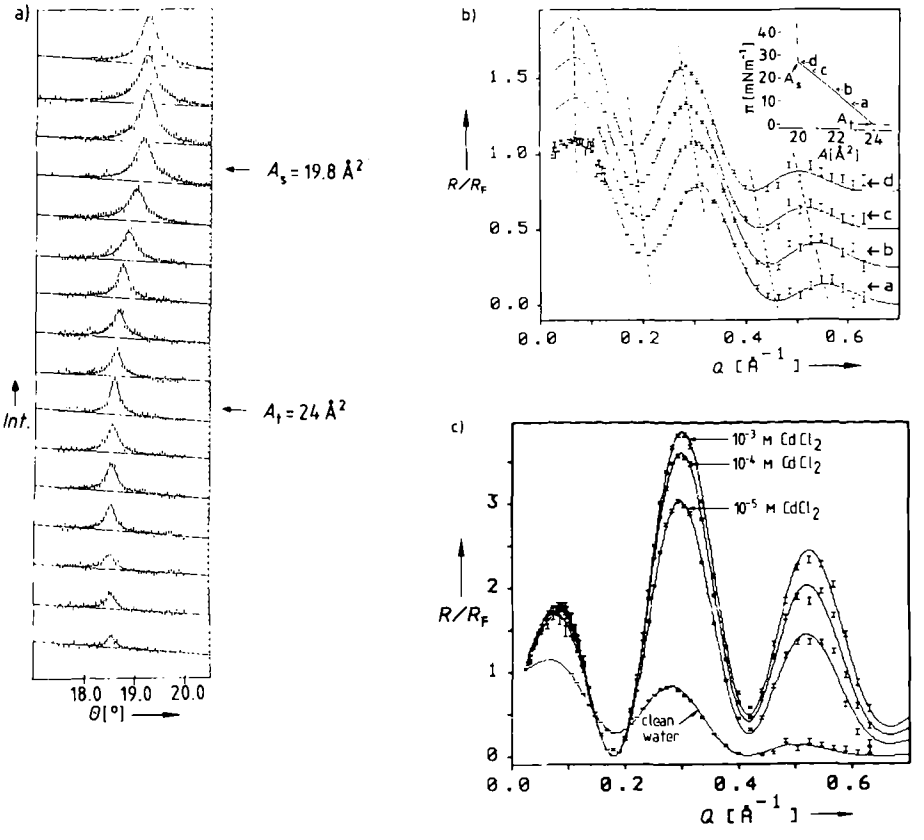

Fig. 4. X-ray scattering data of arachidic acid monolayers at the air/water interface. a) Diffracted intensity as a function of in plane diffraction angle θ for arachidic acid monolayers in the absence of ions and increasing the surface pressure from bottom to top. Indicated are also the areas per molecule A_s, A_t corresponding to breaks in the isotherm slope seen in the insert of b). b) X-ray reflectivity R normalized to the *Fresnel* reflectivity R_F as a function of vertical wave-vector transfer $Q = \frac{4\pi}{\lambda}\sin\alpha$, α being the reflection angle. The lines through the measurement points were obtained from a data fit using the referenced box model. No ions in the subphase, pH 5.5, $T = 20$ °C. The measurements are displaced by 0.25 units along the ordinate and correspond to the points indicated on the isotherm in the insert. c) Reflectivity in the absence and presence (concentration indicated) of $CdCl_2$ in the subphase.

These regimes can be correlated with the pressure/area isotherm given in the insert in Figure 4b and interpreted as follows: I corresponds to the coexistence of an expanded disordered with a compressible ordered phase. One measures diffraction of the ordered phase with area fraction decreasing with pressure. Regime II is ascribed to an ordered phase where the structure varies continuously with surface pressure. III is a much less compressible phase normally called the solid phase.[1]

It is especially interesting to study the structural change in regime II in more detail, and this can be done by analysis of X-ray reflection. The reflection intensity R normalized to the value R_F expected for a stepwise density change R_F, as a function of incidence angle α $\left(Q = \frac{4\pi}{\lambda}\sin\alpha\right)$ is given in Figure 4b for various positions along the isotherm. The curves can be simulated using a box model[6, 27] where the monolayer consists of two different slabs with defined density and thickness. On the water surface there is the slab containing the head groups (carboxy in this case); it is thus of higher electron density than water. A second slab above the first one contains the hydrocarbon tails and thus exhibits lower electron density. Obviously data have to be analyzed by a sensible combination of simulation and molecular modeling. For a more qualitative approach, however, one may use the fact that the first minimum in the reflectivity curve is due to a destructive interference of reflection at the air/hydrocarbon interface with that from the center of the head groups. The corresponding wave vector Q_{min} is therefore related to the lengths of head group and tail, l_H and l_T, respectively, according to

$$Q_{min} \cdot (l_T + l_{H/2}) = \frac{3}{2}\pi \qquad (c)$$

The shift of the minimum in Figure 4b with surface pressure can therefore be understood as an increase in film thickness. A more detailed analysis shows that within regime II the electron density in the tail region is constant and very high.[28] This demonstrates a uniform alignment of aliphatic tails in the all-*trans* configuration. Comparing the film thickness determined (l_T) with that expected for vertical tail orientation (l_T°) one may calculate the tilt angle φ with respect to the surface normal

$$\cos\varphi = \frac{l_T}{l_T^\circ} \qquad (d)$$

From the reflectivity data one then derives a continuous reduction of the tilt angle from about 30° to 0° in reducing the area per molecule from A_t to A_s. Compression of the monolayer therefore enforces a continuous change of the chain tilt and of the lattice constant.

ADVANCED MATERIALS

To demonstrate the high sensitivity of the X-ray technique to monitor the electron density near the interface Figure 4c compares the X-ray reflectivity measured in the absence and presence of different concentrations of $CdCl_2$ in the subphase for a monolayer in the highly condensed state. One realizes the dramatic influence of the counterion which is almost saturated at the lowest concentration used. This influence is basically due to the increase in electron density in the head group moiety by addition of $1/2\,Cd^{2+}$ per head group.

From a line shape analysis one may derive the positional coherence length. Assuming a grain-like structure one may calculate the grain size L/d from the measured line width Δ according to $L/d = 0.443/\Delta$.

In the example presented above one determines $L/d \approx 100$. This is in marked contrast to the coherence length of crystallographic axes (orientational order) which is larger than $10^5 d$, as determined from electron diffraction[23] and fluorescence polarization data.[29] Similar features were also observed for monolayers of phospholipids[4,5] where in addition a phase transition was found with a drastic change in positional coherence length. Phases with long range positional and short range orientational order are expected theoretically for two-dimensional systems.[30] These calculations also showed the strong influence of trapped impurities on the line shape in accordance with our findings.

4. Structure Formation During Adsorption

The ideas discussed in the preceding sections should not only be valid for surfactant monolayers but more generally for two-dimensional structures at interfaces. An example on this is presented in Figure 5. In a subphase containing a negatively charged dye, it is possible to concentrate the dye near the interface by spreading a positively charged monolayer. If the concentration exceeds the solubility limit the dye crystallizes and in the present example may form brightly fluorescing J-aggregates.[31] Varying the subphase and monolayer conditions various crystal morphologies can be prepared[32] and distinguished by polarization microscopy. On spreading and compressing a monolayer, circular patches of nonoriented aggregates are formed (Fig. 5a). These exhibit dimensions and superstructures similar to those of lipid domains. After some minutes recrystallization becomes observable at the boundary of these domains yielding much brighter linear aggregates (Fig. 5a). On expanding the film the domains disappear and on a second compression the linear aggregates dominate (Fig. c, d). These are of very homogeneous size, which is determined by growth conditions, and repel one another similar to the lamellae of Figure 1. Due to the very high order within these domains sharp electron diffraction spots can be observed.[33]

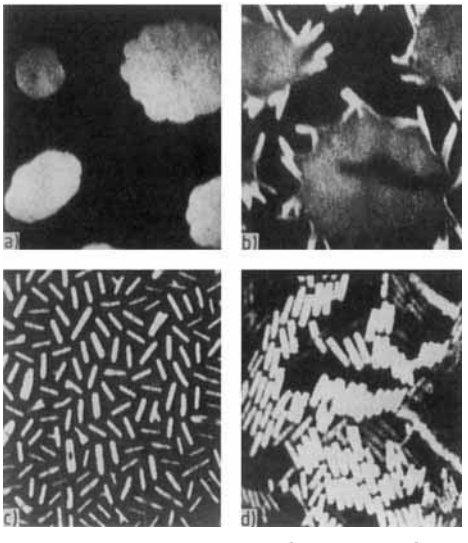

Fig. 5. Fluorescence micrographs of J-aggregates of a water-soluble cyanine dye electrostatically bound to a positively charged monolayer. a) Structure formed immediately after compression and b) about 10 min at a fixed area per molecule. c, d) Second compression with highest molecular density. Different brightnesses are due to the intrinsic polarization of the detection system pH 5.5, $T = 20°C$, the image size corresponds to 150 μm.

5. Proteins in Thin Films

It has been shown that proteins can be arranged and distributed in a monolayer in a similar way as staining dyes.[34,35] They are generally less soluble in the more condensed phase and therefore concentrated in the fluid environment. This opens new possibilities for increasing local concentrations of reactants and thus to enhance reaction rates. One step further along this line may be to increase protein concentrations at boundaries.

As an example of the latter, Figure 6 presents fluorescence micrographs showing the distribution of fluores-

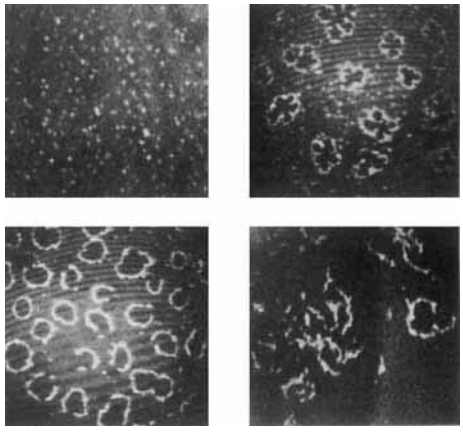

Fig. 6. Fluorescence micrograph of a DMPE monolayer containing aggregated fluorescently labeled Con A. Protein patches already present in the fluid monolayer phase (upper left) are attracted to the fluid/solid domain boundary when the monolayer is in the phase coexistence range (upper right and lower left). On reexpansion the solid (darkest) DMPE domains melt leaving strings of protein (lower right) $T = 20°C$, pH 7, 100 μM $MnCl_2$, 100 μM $CaCl_2$, 100 mM NaCl.

cently labeled Concanavalin A (Con A) in a DMPE monolayer in the phase coexistence range. One clearly observes the condensed phase DMPE domains (dark) surrounded by a frame of protein patches in those images except in that on the top left where the complete monolayer is fluid. The arrangement of these patches can be understood as follows: According to surface potential data the protein has a normal dipole moment opposite to that of the lipid.[36] Its patches are therefore attracted by the condensed phase domains. Due to the dense packing of the latter, however, they are not incorporated in these domains and therefore remain near the boundary. The protein boundary is a rather loose structure and allows lipid penetration to the interface, since the DMPE domains continue to grow on further compression. On the other hand, on expansion of the monolayer the DMPE domains melt, but the protein patches remain connected to form strings.[37]

6. Concluding Remarks

It is now possible to produce ultrathin films with a periodic arrangement of functional molecules like dyes or proteins. Such control, on an almost molecular level, is a central requirement for any future device fabrication. New ways and physical principles to achieve this were described in this article. Our studies were performed with compounds similar to biological systems. The systems may be considered too artificial by a biologist and too biological by a materials scientist. Nevertheless I tried to demonstrate that part of the ideas presented may be applicable to seemingly different systems like adsorbates or to the fabrication of biosensors requiring oriented arrays of receptor proteins. Beyond that, there are many serious attempts to use this class of organic films for optical, optoelectronic, lubrication, lithographic and other applications, all requiring microstructure control. This report should primarily stimulate more elaborate experimental as well as theoretical studies.

Received: February 11, 1988

[1] G. Gaines: *Insoluble Monolayers at Liquid-Gas Interfaces*, Interscience, New York 1966.
[2] H. Kuhn, D. Möbius, *Angew. Chem. 83* (1971) 672; *Angew. Chem. Int. Ed. Engl. 10* (1979) 620.
[3] M. Lösche, H. Möhwald, *Rev. Sci. Instrum. 55* (1984) 1968.
[4] K. Kjaer, J. Als-Nielsen, C. A. Helm, L. A. Laxhuber, H. Möhwald, *Phys. Rev. Lett. 58* (1987) 2224.
[5] C. A. Helm, H. Möhwald, K. Kjaer, J. Als-Nielsen, *Biophys. J. 52* (1987) 381.
[6] C. A. Helm, H. Möhwald, K. Kjaer, J. Als-Nielsen, *Europhys. Lett. 4* (1987) 697.
[7] K. Kjaer, J. Als-Nielsen, C. A. Helm, P. Tippmann-Krayer, H. Möhwald, *Thin Solid Films*, in press.
[8] A. Fischer, E. Sackmann, *J. Colloid Interface Sci. 112* (1986) 1.
[9] O. Albrecht, H. Gruler, E. Sackmann, *J. Physique 39* (1978) 301.
[10] C. A. Helm, L. A. Laxhuber, M. Lösche, H. Möhwald, *Colloid Polym. Sci. 264* (1986) 46.
[11] A. Miller, C. A. Helm, H. Möhwald, *J. Phys. (Les Ulis, Fr.) 48* (1987) 693.
[12] A. Fischer, E. Sackmann, *J. Phys. (Les Ulis, Fr.) 45* (1984) 517.
[13] D. Andelman, F. Brochard, J.-F. Joanny, *J. Chem. Phys. 86* (1987) 2673.
[14] A. Miller, H. Möhwald, *Europhys. Lett. 2* (1986) 67.
[15] M. Lösche, H.-P. Duwe, H. Möhwald, *J. Colloid Interface Sci.*, in press.
[16] C. A. Helm, H. Möhwald, *J. Phys. Chem.*, in press.
[17] W. M. Heckl, M. Lösche, D. A. Cadenhead, H. Möhwald, *Eur. Biophys. J. 14* (1986) 11.
[18] W. M. Heckl, H. Möhwald, *Ber. Bunsenges. Phys. Chem. 90* (1986) 1159.
[19] A. Miller, H. Möhwald, *J. Chem. Phys. 86* (1987) 4258.
[20] H. D. Göbel, H. E. Gaub, H. Möhwald, *Chem. Phys. Lett. 138* (1987) 441.
[21] A. Miller, W. Knoll, H. Möhwald, *Phys. Rev. Lett. 56* (1986) 2311.
[22] J. Nittman, H. E. Stanley, *Nature (London) 321* (1986) 663.
[23] A. Fischer, M. Lösche, H. Möhwald, E. Sackmann, *J. Phys. Lett. 45* (1984) 785.
[24] H. D. Göbel, H. Möhwald, *Thin Solid Films*, in press.
[25] C. Duschl, W. Frey, W. Knoll, *Thin Solid Films*, in press.
[26] A. Barraud, M. Flörsheimer, H. Möhwald, J. Richard, A. Ruaudel-Teixier, M. Vandevyver, *J. Colloid Interface Sci.*, in press.
[27] J. Als-Nielsen in W. Schommers, P. Blanckenhagen (Eds.): *Structure and Dynamics of Surfaces, Vol. 2*, Springer, Berlin 1986, Chapter 5.
[28] K. Kjaer, J. Als-Nielsen, C. A. Helm, P. Tippmann-Krayer, H. Möhwald, unpublished.
[29] V. T. Moy, D. Keller, H. E. Gaub, H. M. McConnell, *J. Phys. Chem. 90* (1986) 3198.
[30] D. R. Nelson, M. Rubinstein, F. Spaepen, *Phil. Magn. A 46* (1982) 105.
[31] M. Shimomura, T. Kunitake, *J. Am. Chem. Soc. 109* (1987) 5175.
[32] S. Kirstein, *Diplomarbeit*, Technische Universität München 1988.
[33] R. Steitz, *Diplomarbeit*, Universität Mainz 1988.
[34] W. M. Heckl, H. Möhwald, *J. Mol. Electron. 3* (1987) 67.
[35] J. Peschke, H. Möhwald, *Colloids Surf. 27* (1987) 305.
[36] W. M. Heckl, M. Thompson, H. Möhwald, *J. Am. Chem. Soc. 110* (1988), in press.
[37] H. Haas, *Diplomarbeit*, Universität Mainz 1988.